Metallodendritic catalysis

Dendrimer-encapsulated metal nanoparticles and their applications to catalysis

Yanhui Niu, Richard M. Crooks *

Department of Chemistry, Texas A&M University, P.O. Box 30012, College Station, TX 77842–3012, USA

Abstract

This account describes the synthesis, characterization, and applications to catalysis of dendrimer-encapsulated metal nanoparticles (DEMNs). These materials are synthesized by a template approach in which metal ions are sorbed into the interior of dendrimers and then subsequently chemically reduced to yield nearly size-monodisperse, zero-valent metal particles having dimensions of less than 4 nm. The dendrimer component of these composites serve not only as a template for preparing the nanoparticle replica, but they also stabilize the nanoparticle, make it possible to tune solubility, and enhance catalytic selectivity. These materials have been used for a broad range of catalytic reactions, including hydrogenations, Heck coupling, and Suzuki reactions, in water, organic solvents, biphasic fluorous/organic solvents, and supercritical CO_2. In many cases it is very simple to recycle the dendrimer-encapsulated catalysts. In addition to monometallic DEMNs, bimetallic materials have also recently been prepared and their catalytic properties are reported. ***To cite this article: Y. Niu et al., C. R. Chimie 6 (2003).***

1. Introduction

This account reports recent developments related to the catalytic properties of dendrimer-encapsulated metal nanoparticles (DEMNs). Particular emphasis is placed on specific functions and properties of these materials that are a direct consequence of their dendritic architecture.

Dendrimers are well-defined, three-dimensional polymers synthesized by a divergent or convergent method[1]. Since the first report of a dendrimer synthesis in 1978 [2], there has been increasing interest in

developing new structures, syntheses, and applications for these fascinating materials [1,3–10]. As a consequence of their unique structural topology and chemical versatility, dendrimers have found (or are likely to find) applications that include catalysis [3,5,7], drug delivery [11,12], energy transfer [13–15], and molecular recognition [6,16].

Among the potential applications for dendrimers, catalysis may be one of the most promising, because it is relatively easy to tune the structure, size, and location of catalytically active sites [3], and because dendrimers have the potential to combine the advantages of both heterogeneous and homogeneous catalysts [7]. An enormous variety of catalytic reactions involving composite metal-dendrimer materials have been stud-

* Corresponding author.
E-mail address: crooks@tamu.edu (R.M. Crooks).

ied; these include, but are not limited to, hydrogenations, hydroformylation, olefin metathesis, Heck reactions, Suzuki coupling, alkylation, and oxidations. The properties of dendrimer-based catalysts, such as selectivity, activity, and stability, are dependent on the location and nature of the metal. Fig. 1 is a schematic illustration of the four most common metallodendrimer configurations. This review focuses exclusively on dendrimer-encapsulated metal nanoparticles (Fig. 1a), and particularly their catalytic properties. Excellent reviews about dendrimers having catalytically active metal sites on the periphery (Fig. 1b) [17], at the core (Fig. 1c), and at the branch points (Fig. 1d) are available [18–20].

We [5,21] and others [22–25] have previously reported the synthesis of dendrimer-encapsulated monometallic, bimetallic [26], and semiconductor [27] nanoparticles (Fig. 1a). Nearly monodisperse intradendrimer nanoparticles having sizes of less than 4 nm (depending on the size of the dendrimer) can be prepared. Dendrimers are particularly attractive hosts for catalytically active metal nanoparticles for the following five reasons: (1) bearing fairly uniform composition and structure, the dendrimer templates themselves
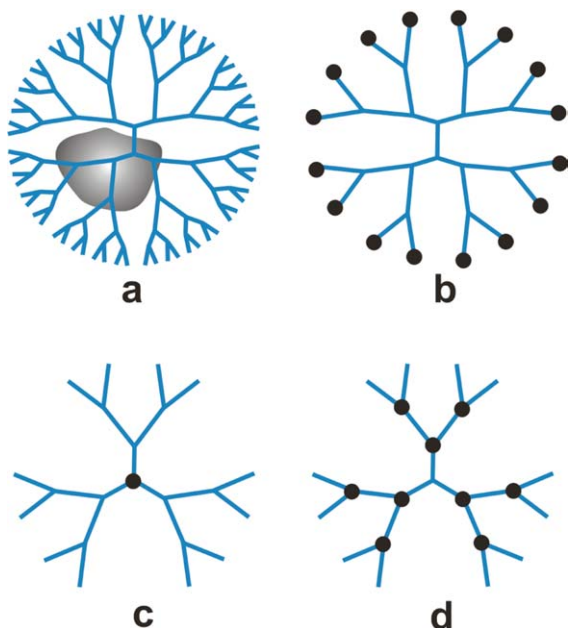
yield well-defined nanoparticle replicas; (2) the nanoparticles are stabilized by encapsulation within the dendrimer, and therefore they do not agglomerate during catalytic reactions; (3) the nanoparticles are retained within the dendrimer primarily by steric effects and therefore a substantial fraction of their surface is unpassivated and available to participate in catalytic reactions; (4) the dendrimer branches can be used as selective gates to control the access of small molecules (substrates) to the encapsulated (catalytic) nanoparticles; (5) the dendrimer periphery can be tailored to control solubility of the hybrid nanocomposite and used as a handle to facilitate linking to surfaces and other polymers.

One significant advantage of DEMNs over the other three types of metallodendrimer catalysts shown in Fig. 1 is that the necessary poly(amidoamine) (PAMAM) and poly(propylene imine) (PPI) dendrimers are commercially available – both dendrimers can be purchased from Aldrich Chemical Co. (Milwaukee, WI): PAMAM dendrimers are produced by Dendritech, Inc. (Midland, MI), PPI dendrimers are produced by DSM Fine Chemicals (The Netherlands). Solubility of these commercially available materials can be easily tuned by modification of the peripheral functional groups [8] or by using biphasic solvents.

2. Synthesis and characterization of DEMNs

Dendrimer/metal-ion composite materials, which are the precursors for DEMNs, are prepared by mixing solutions containing dendrimers and metal ions, such as Pt^{2+}, Pd^{2+}, Au^{3+}, Ag^+, Cu^{2+}, Ni^{2+}, Ru^{3+}, Mn^{2+}, and Fe^{3+} (Fig. 2) [5,22,23,25,28,29]. The reaction is usually carried out in water, but as described later organic solvents have also been used. PAMAM dendrimers having non-complexing peripheral functional groups have been used extensively for this purpose, but other types of dendrimers have also been studied [30,31]. In

Fig. 1. Types of metallodendrimers: (**a**) dendrimer-encapsulated metal nanoparticles (DEMNs), (**b**) dendrimers modified on the periphery with metal ions or complexes, (**c**) core metallodendrimers, (**d**) focal-point metallodendrimers. Figure adapted from [3].
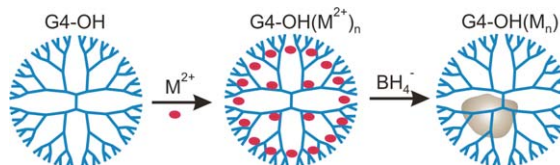

Fig. 2. Schematic representation of the synthesis of dendrimer-encapsulated metal nanoparticles (DEMNs).

favorable cases the metal ions partition into the dendrimer interior where they complex strongly with interior tertiary amine groups. UV-vis, EPR, MALDI-MS, and XPS have been used to characterize dendrimer/metal-ion composites [21,28,29,32–34]. In the case of the PAMAM/Cu^{2+} composite [21], for example, a strong ligand-to-metal charge transfer (LMCT) band at 300 nm and a 210 nm shift of the d-d optical transition signal metal ion complexation by the interior amine groups. The maximum number of Cu^{2+} ions that can be extracted into each dendrimer is related to the dendrimer generation and has been assessed by spectrophotometric titrations [21].

To successfully extract metal ions into the interior of dendrimers having complexing peripheral groups, such as amine-terminated dendrimers, the solution pH may play an important role. This is because PAMAM dendrimers are polyprotic bases where the surface primary amines (pK_a = 9.23) are more basic than the internal tertiary amines (pK_a = 6.30) [35]. Results from calculations based on a multi-shell model provide insight into dendrimer protonation over a broad range of pH [35,36]. Acidic conditions have been shown to be effective for trapping metal ions within the interior of amine-terminated dendrimers while avoiding coordination of metal ions to primary amine groups on the periphery [37].

Reduction of dendrimer/metal-ion composites with an excess of a chemical reducing agent (usually $NaBH_4$) in water yields nearly monodisperse, zerovalent intradendrimer metal nanoparticles (Fig. 2). Reduction is apparent from the immediate change in color of the solution. In the case of Cu, for example, the UV–vis spectrum changes from the aforementioned pair of discrete bands prior to reduction to a monotonically increasing absorbance toward shorter wavelength, indicating the presence of small nanoparticles. The absence of an absorption peak arising from Mie plasmon resonance indicates that the Cu clusters are smaller than 4 nm [38,39]. Consistent with this observation, no precipitation of metal occurs.

High-resolution transmission electron microscopy (HRTEM) is widely used to study the size and size distribution of metal nanoparticles. HRTEM clearly shows that DEMNs are typically in the size range of 1–4 nm [22,32,33,40,41]. The particle size can be controlled by varying the dendrimer/metal-ion ratio. For example, we have shown that a dendrimer/$PdCl_4^{2-}$

ratio of 1:40 yields Pd nanoparticles having a diameter of 1.7 ± 0.2 nm regardless of the dendrimer generation (Gn–OH dendrimers [n = 4, 6, and 8]) [40] or steric crowding on the dendrimer surface (Fig. 3) [42]. Note, however, that the size of a spheroidal particle containing 40 close-packed Pd atoms should be ~1.1 nm in diameter. That is, TEM over-estimates the size of small Pd DEMNs contained within low-generation PAMAM dendrimers by more than 50% in some cases [5,32,41]. Consistent with the relatively limited void space within low-generation PAMAM dendrimers, this result might indicate that DEMNs prepared under these conditions have complex shapes. In contrast, the measured size of large Au nanoparticles (2.0–4.0 nm) encapsulated within high-generation (G6–G9) PAMAM dendrimers correlates well with the calculated size of spheroidal nanoparticles [22]. Additionally, our group recently showed that when DEMNs are prepared using a magic number [43,44] (or close to a magic number) of metal ions (for example, a dendrimer/$AuCl_4^-$ ratio of 1:140), the size of the resulting nanoparticles (1.6 ± 0.3 nm for a ^{140}Au-atom particle, Fig. 4) [45] matches the theoretical expectation (1.6 nm) very well, even for low-generation dendrimers [44] – the dendrimers used in this study were quaternized sixth-generation PAMAM dendrimers [46]. This is because magic numbers of atoms lead to favorable, low-energy nanoparticle structures. Moreover, the degree of monodispersity obtained using magic numbers is truly remarkable. Gröhn and co-workers have used TEM staining methods and scattering data to demonstrate that Au DEMNs are encapsulated within high-generation dendrimers and that the location of the nanoparticles are, on average, somewhat offset from the center of PAMAM dendrimers [22]. The shape and location of encapsulated metal nanoparticles will be discussed later in this chapter.

DEMNs soluble in non-aqueous solvents have also been synthesized. For example, we recently demonstrated that Pd particles within water-soluble, amine-terminated PAMAM dendrimers can be transported into an organic phase or a fluorous phase by addition of a fatty acid [37] or a perfluorinated fatty acid, respectively [47]. It is also possible to extract metal ions from an aqueous phase into a non-aqueous phase [48], and then reduce the ions to the zero-valent metal in the non-aqueous phase. Esumi et al. used this approach to prepare dendrimer-encapsulated Au nanoparticles within PAMAM dendrimers carrying hydrophobic
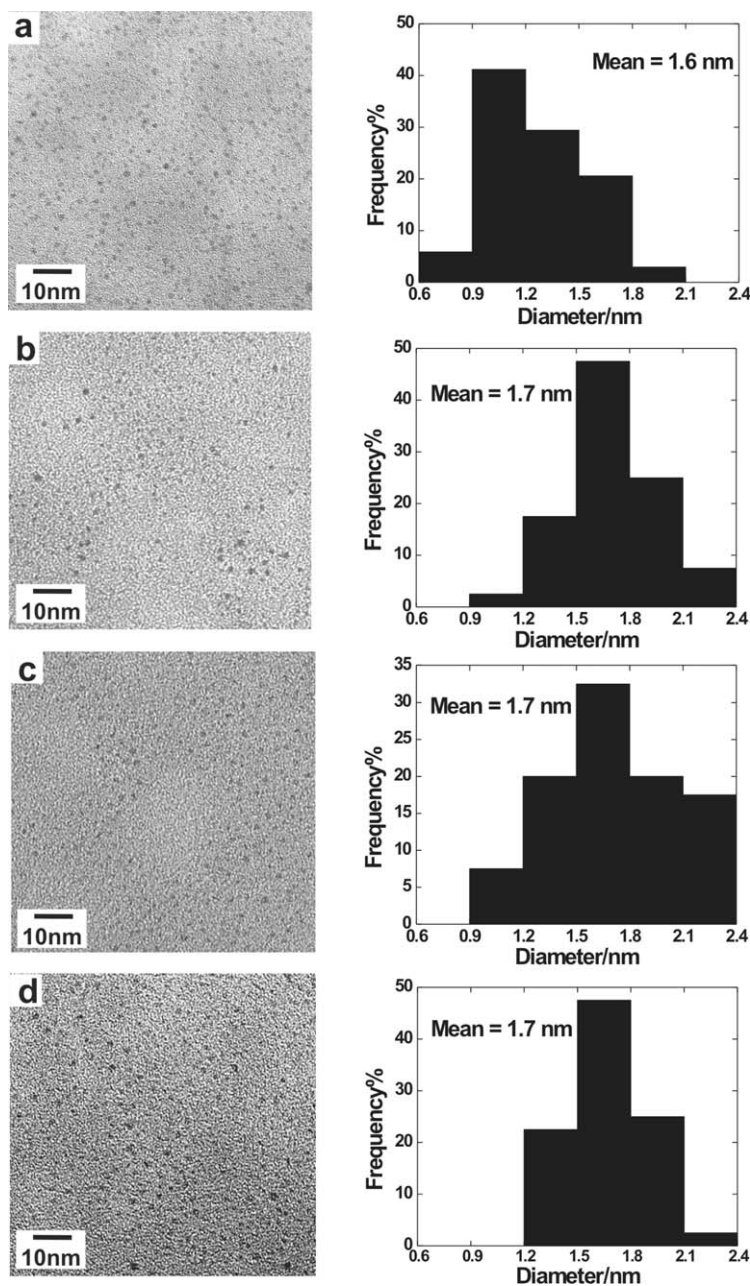
Fig. 3. TEM images and particle size distributions for (**a**) G4-OH/Pd(0)$_{40}$, (**b**) G4-EP1/Pd(0)$_{40}$, (**c**) G4-EP2/Pd(0)$_{40}$, and (**d**) G4-EP3/Pd(0)$_{40}$ catalysts. G4-EP*n* represents modified fourth-generation PAMAM dendrimers having different α-aminoalcohols on the periphery (see Fig. 7).

groups on their periphery [49]. We later showed that this strategy can be used to prepare fluorous-soluble DEMNs [50]. It is also possible to completely avoid the extraction process by preparing DEMNs in the absence of water. This is accomplished by first sorbing

the metal ions into the dendrimer interior in a non-aqueous solvent, and then reducing the composite [51,52]. Our results suggest that it is possible to use this approach to encapsulate larger metal nanoparticles within dendrimers, because the main driving force for
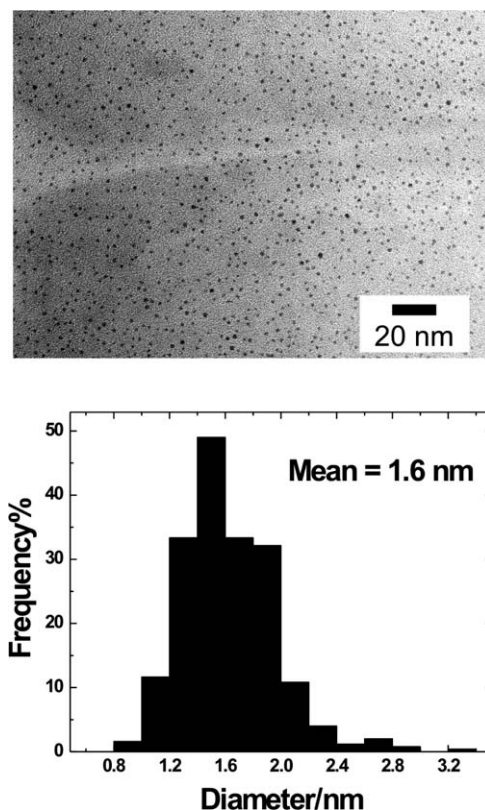
Fig. 4. TEM images and Au particle-size distributions for a sixth-generation PAMAM dendrimer having 50% of the functional groups on the periphery functionalized with quaternary amines (G6-AC/Au(0)$_{140}$). The dendrimer was synthesized via the reaction between G6-NH$_2$ and glycidyltrimethylammonium chloride (1:1 mol ratio) at 40 °C in methanol. After evaporation of the solvent, the quaternized G6-AC dendrimer was dissolved in H$_2$O followed by dialysis against H$_2$O. NMR and MALDI–MS confirmed 50% of surface groups on the dendrimer were quaternary amines.

encapsulation is the difference in metal-ion solubility between the solvent and the interior of the dendrimer [52]. This approach greatly expands the scope of our previously reported strategy for preparing DEMNs in water. Finally, we have also shown that it is possible to extract metal particles from within the interior of dendrimers, and transport them into an organic phase as ligand-stabilized clusters [53].
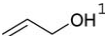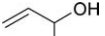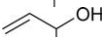
3. Homogeneous catalysis using DEMNs

Because the active sites of metal catalysts are on the particle surface, smaller metal particles are, on a per-atom basis, usually more efficient than larger particles

(exceptions to this generality exist, particularly for nanoparticles in the 1–3 nm size range) [54]. However, the high total surface energy of small particles is also a strong driving force for aggregation. This negative consequence of small-sized particles can be avoided by adding stabilizers to the metal-ion solution prior to reduction. The stabilizers sorb to the surface of the growing particles and lower their surface energy, thereby reducing the likelihood of aggregation and precipitation [55,56]. Reduction of the corresponding ions in the presence of monomeric amphiphiles, such as thiols [57,58] or detergents [59], or polymers [60,61], results in formation of stabilized nanoparticles. For homogeneous catalysis, however, complete and irreversible adsorption of stabilizers is undesirable, because all active sites on the particle surface are poisoned, which in turn leads to loss of catalytic activity. Clearly, synthesis of highly efficient nanoparticle catalysts requires optimization of both the particle size and the surface protective chemistry.

Because DEMNs are, at least to some extent, sterically retained within dendrimers, a significant fraction of their surface is unpassivated and thus available for catalysis. Furthermore, DEMNs can be used as homogeneous catalysts in almost any solvent, because the host dendrimers can be tailored for specific solvents. For example, hydroxyl-terminated, fourth-generation PAMAM dendrimers containing 40-atom Pd nanoparticles (G4-OH(Pd$_{40}$)) efficiently catalyze the hydrogenation of both linear and branched alkenes in aqueous solution [32]. DEMNs have also been used to catalyze Suzuki cross-coupling reactions between arylboronic acids and aryl halides in water [41]. In this study G3-OH(Pd$_{10}$) was shown to be more efficient for coupling phenylboronic acid and iodobenzene than G4-OH(Pd$_{10}$), but G3-OH(Pd$_{10}$) was found to be less stable. This is a consequence of the relative openness of the dendritic architecture: more open architectures permit more facile ingress and egress of substrates and products, but they are not as robust for stabilization.

Solvent plays an important role in the rate of DEMN-catalyzed hydrogenation reactions. For example, the TOFs for the hydrogenation of allyl alcohol in water using G4-OH(Pd$_{40}$), G6-OH(Pd$_{40}$), and G8-OH(Pd$_{40}$) catalysts are 220, 200, and 130 mol H$_2$(mol Pd)$^{-1}$ h^{-1}, respectively [32,40]. In contrast, the maximum TOFs for allyl alcohol hydrogenation in a mixed MeOH–H$_2$O (4:1, v/v) solvent are greater by about a

Table 1
Hydrogenation reaction rates using Gn-OH/Pd(0)40 catalysts for structurally related allyl alcohol and allylic alcohols

Substrates	TOF[mol H_2(mol Pd)$^{-1}$ h^{-1}]		
	G4-OH(Pd40)	G6-OH/Pd(0)40	G8-OH/Pd(0)40
⟋⟍OH[1]	480/470[2]	450/460[2]	120
⟋⟍⟍OH[1]	220[1]	200[1]	130[1]
⟋⟍⟍OH	450/460[2]	380	93
⟋⟍⟍OH	260	280	68
⟋⟍⟍OH	150	75	62
⟋⟍⟍OH	100	40	50

Hydrogenation reactions were carried out at 25 ± 2 °C using 2×10^{-4} M Pd(0) composite catalysts in MeOH–H_2O (4:1 v/v) mixtures. The turnover frequency (TOF) was calculated based on H_2 uptake (mol H_2 (mol Pd[0] h)$^{-1}$).

[1] Hydrogenation reactions were carried out at 25 ± 2 °C using 2×10^{-4} M Pd(0) composite catalysts in water only (no methanol).

[2] Duplicate measurements were performed to illustrate the level of run-to-run reproducibility.

factor of two for G4-OH(Pd$_{40}$) and G6-OH(Pd$_{40}$), but nearly the same for G8-OH(Pd$_{40}$) (Table 1) [40]. It is possible that the increased solubility of hydrogen in methanol [62,63], changes in the surface chemistry of the encapsulated Pd nanoparticles, structural changes of the dendrimer template driven by differences in solvent polarity, or enhanced partitioning of the substrate into the dendrimer in the mixed solvent [64,65] are responsible for this finding, but a clear understanding awaits a comprehensive study.

In addition to water and mixed water-alcohol phases, we have also tested the catalytic activities of DEMNs in pure organic solvents. For example, after being extracted from water into toluene as monodisperse inverse micelles by a surfactant (dodecanoic acid), Pd nanoparticles encapsulated within fourth-generation, amine-terminated (G4-NH$_2$) PAMAM dendrimers exhibited better hydrogenation activity for allyl alcohol than was observed in water [37]. We attribute this finding to the relatively hydrophilic interior of the PAMAM dendrimer molecule, which may facilitate partitioning of the substrate into the vicinity of the encapsulated nanoparticle.

Supercritical CO_2 (scCO_2) is an important solvent, because it has easily tunable solvent properties and because it is nontoxic [66]. We recently showed that Pd nanoparticles encapsulated within perfluorinated dendrimers are soluble in scCO_2, and that they catalyze Heck coupling. Interestingly, we found that coupling of aryliodides and methacrylate yields the highly unfavorable 2-phenylacrylic acid methyl ester isomer, rather than the preferred trans-cinnamaldehyde [67]. This finding suggests that judicious tuning of solvent conditions, dendrimer structure, and catalyst composition may provide a means for enhancing product selectivity.

4. Size-selective catalysis using dendrimer-encapsulated catalysts (DECs)

We recently developed an approach for using dendrimers as size-selective nanofilters to control access of small molecules to the dendrimer interior. This provides another means for introducing selectivity to an intrinsically nonselective catalyst [40]. We hypothesized that dendrimer generations could be used to size-select substrates, because higher generation dendrimers have more crowded peripheries, which limit access of the substrate to the encapsulated nanoparticle (Fig. 5). To test this idea, we prepared dendrimer-encapsulated nanoparticles containing an average of 40 Pd atoms within the interior of three different generations of Gn–OH dendrimers (*n* = 4, 6, 8). This results in a homologous series of DECs in which only the porosity and diameter of the dendrimer vary. The hydrogenation rates of chemically similar, but structurally different, allyl alcohol and four allylic alcohol derivatives (**1–5**, Table 1) having different sizes and shapes were then measured to test the aforementioned hypothesis.

The results indicate that the hydrogenation turnover frequency (TOF) decreases as the substrate size increases for a particular DEMN, while for a specific substrate the TOF decreases as the dendrimer size increases (Table 1). However, hydrogenation of these same alcohols showed no significant difference in reaction rate when a nonselective Pd/C catalyst was used. Hydrogenation products were identified by NMR spectroscopy.

Molecular modeling was used to better understand these experimental findings. The distance between ad-
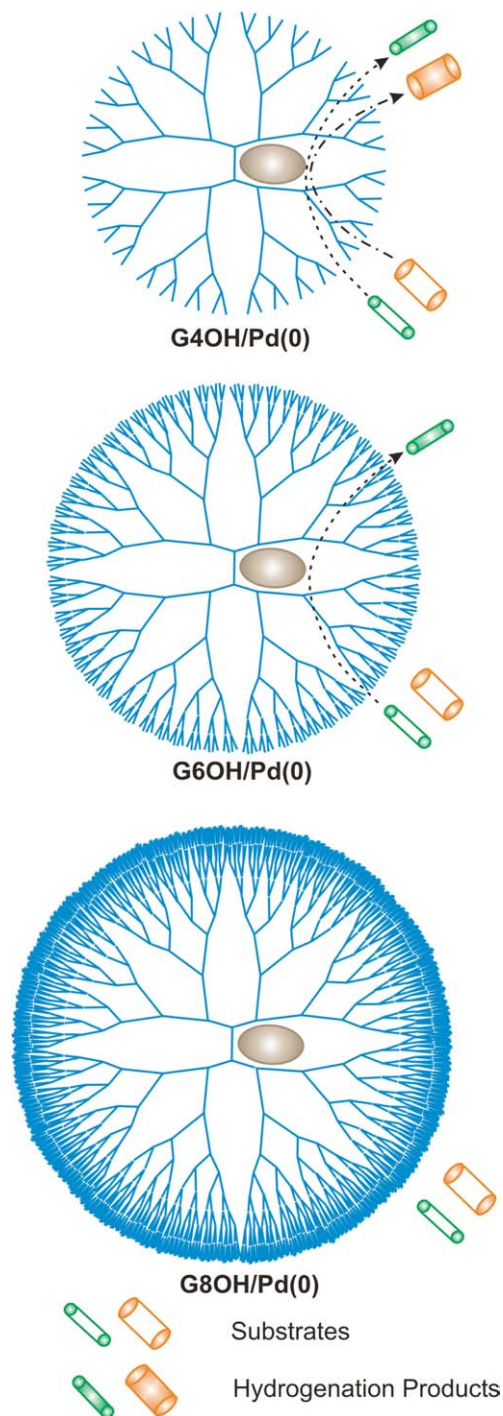
Fig. 5. Schematic representation of size-selective hydrogenation by DEMNs prepared within different generation dendrimers. Reprinted with permission from J. Am. Chem. Soc. 123 (2001) 6840–6846. © 2001 American Chemical Society.

jacent terminal groups for the different generation dendrimers was calculated using appropriate molecular models and reasonable assumptions [40]. The calculated average edge-to-edge van der Waals distance between two terminal hydroxyl groups in G4-OH, G6-OH, and G8-OH are 8.2, 5.4, and 3.2 Å, respectively. These values can be compared to the largest linear dimension perpendicular to the O-H bond for substrates **1–5**, which are 5.5, 7.0, 7.5, 7.0, and 8.0 Å, respectively. The correspondence between these values and the experimental data in Table 1 suggests that the hypothesis in Fig. 5 provides a good preliminary model for understanding the relationship between the 'mesh size' of the dendrimer 'nanofilter' and the performance of these dendrimer-based catalysts. A competitive hydrogenation reaction between the smallest (**1**) and largest (**5**) substrates in Table 1 confirms the high degree of selectivity exhibited by dendrimer-encapsulated catalysts. Specifically, ^{1}H NMR spectra of the reaction mixture of **1** and **5** (present at 1:1 mol equiv) before and after treatment with H_2 were recorded as a function of time using G4–OH(Pd$_{40}$) as the catalyst (Fig. 6). The results indicate that the smaller substrate reacts much more quickly than the larger one. Moreover, the relative rates are in excellent agreement with results obtained in noncompetitive experiments (Table 1).
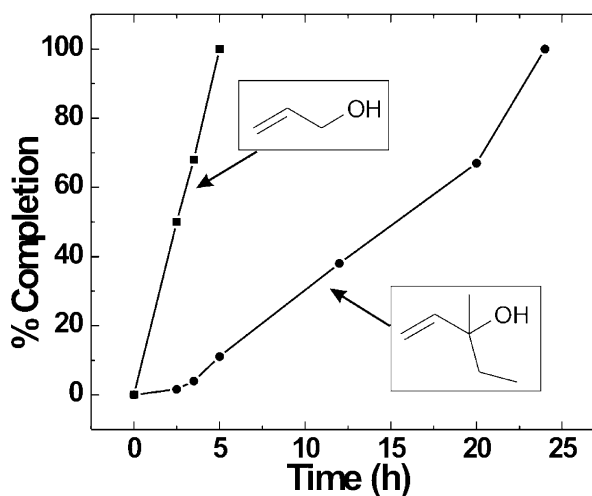

Fig. 6. Plots of the percentage completion of hydrogenation reactions obtained from a CD_3OD:D_2O (4:1, v/v) solution containing 1 M allyl alcohol and 1 M 3-methyl-1-penten-3-ol as a function of time. The solution contained 5×10^{-6} M G4-OH(Pd$_{40}$) and the reaction was carried out at 25 ± 2 °C.
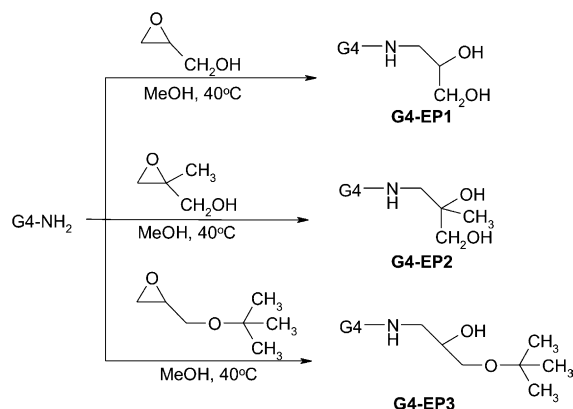
Fig. 7. Synthetic approach for covalently linking α-aminoalcohol groups to the periphery of G4–NH$_2$ PAMAM dendrimers.

To further investigate the effect of dendrimer structure on catalytic selectivity, we investigated the effect of steric crowding on the periphery for a particular generation dendrimer. Fourth-generation PAMAM dendrimers terminated with α-aminoalcohol groups were synthesized for this study (G4-EPn, n = 1–3) by reaction of G4–NH$_2$ with the corresponding epoxide (Fig. 7) [42]. Characterization of these materials using ^{1}H NMR, ^{13}C NMR and MALDI–MS confirmed the formation the dendrimers, and TEM micrographs confirmed that it was possible to prepare encapsulated Pd nanoparticles having diameters of 1.7 ± 0.2 nm (Fig. 3). The specificity of these composite catalysts was then determined for the hydrogenation of allyl alcohol and a series of α-allylic alcohols. The results revealed a clear trend supporting the previously proposed model: increasing steric crowding on the dendrimer periphery (G4–OH < G4–EP1 < G4–EP2 < G4–EP3) resulted in lower TOFs.

5. Molecular rulers as in-situ reporters of DEMNs

A key question raised in the previously described catalysis studies concerns the size, shape, and location of the encapsulated nanoparticles. Gröhn and coworkers used TEM and scattering methods to place Au nanoparticles somewhat offset from the center of Gn–NH$_2$ (n = 6–9) PAMAM dendrimers [22] However, interpretation of data from these methods, and correlation of the results to the conformation of solution-phase dendrimers, is complex and model dependent. For example, TEM imaging necessitates that the dendrimers be stained and placed under vacuum or in frozen solutions [68], all of which distort the shape of the dendrimer [69,70]. Likewise, scattering data for DEMNs have been interpreted by assuming that the encapsulated nanoparticles are spherical [22], but this assumption is also approximate. For example, we have found that TEM over-estimates the size of DEMNs by more than 50% in some cases [5,32]. This and, as mentioned earlier, the high degree of steric crowding within the dendrimer interior, suggests that encapsulated nanoparticles may have complex shapes.

We developed an *in-situ* method for determining the average distance between the surface of dendrimer-encapsulated Pd nanoparticles and the periphery of G4–OH hosts. The advantage of measuring the dendrimer-periphery-to-metal-surface distance *in situ*, is that it is unnecessary to make assumptions about the nanoparticle or dendrimer size and shape. The measurements were made using molecular rulers consisting of three parts: a catalytically active probe (an alkene in this case) at the distal terminus that may undergo a hydrogenation reaction upon contact with the encapsulated catalyst; a large molecular 'stopper' at the proximal end that is unable to enter the host (here, a monosubstituted [β-cyclodextrin (β-CD]); and intervening alkyl chains having different lengths that tether the probe to the stopper and which therefore define the maximum extension of the ruler (Fig. 8) [71].

The time necessary to hydrogenate these molecular rulers was monitored by ^{1}H NMR, and this information was then used to estimate the average location of the encapsulated Pd nanoparticles ($D_{Pd–D}$, Fig. 8). The key finding is that the shortest ruler, mono-6-deoxy-6-(allylamino)cyclodextrin (**R1**, 0.5 nm in length), had the slowest reaction rate while the two longer rulers (**R5** and **R9**, 0.9 and 1.3 nm long, respectively) reacted substantially faster. In contrast, very similar reaction rates were observed for the three rulers when intrinsically nonselective carbon-supported Pd (Pd/C) catalysts were used. Interpretation of the data indicates that the surface of the encapsulated nanoparticle is situated 0.7 ± 0.2 nm from the surface of the dendrimer. Like previously reported TEM and SAXS data, however, the conclusions reported here rely on several assumptions. A reliable, high-resolution picture of the size, shape, and location of DEMNs is still not attainable.
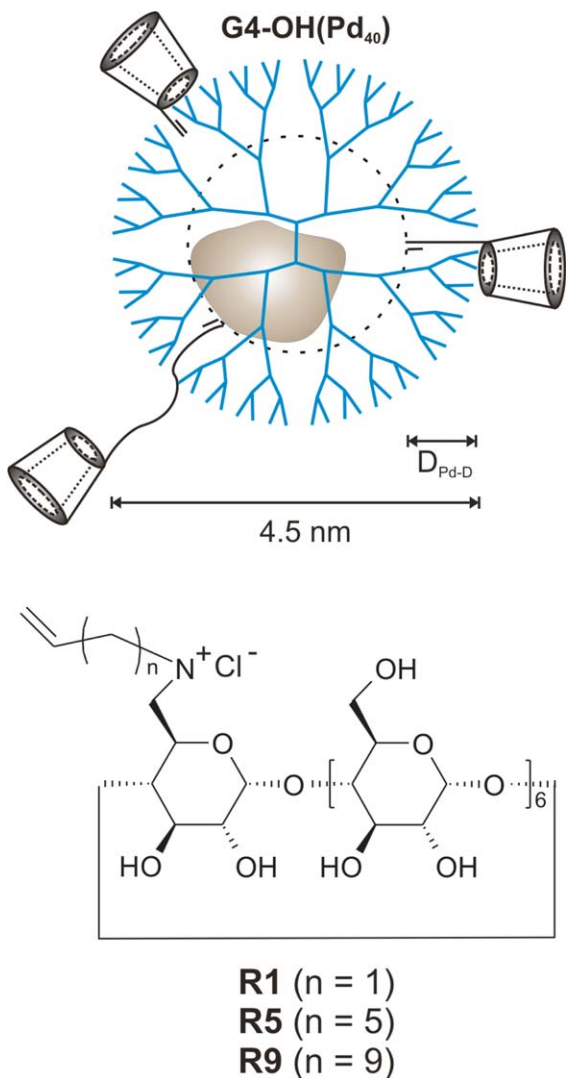
Fig. 8. Top: Schematic representation of the use of molecular rulers to probe the structure of G4–OH(Pd$_{40}$) DEMNs. Bottom: structure of the three rulers discussed in the text.

6. Recycling DEMNs

Invention of strategies for recycling homogeneous catalysts is an important challenge. Recently, new methods, such as the use of biphasic solvents [72,73], supercritical fluids [66,74,75], and nanofiltration [76], have been developed for this purpose. A few examples of methods that have been used to recycle DEMNs are summarized next.

Reactions in biphasic fluorous/organic solvents have demonstrated advantages for recycling of soluble

homogeneous catalyst [72]. We used this approach for hydrogenation and Heck reactions using DEMNs. Non-covalent ion-pairing interactions between the surfaces of PAMAM dendrimers and perfluoroether groups solubilize Pd DEMNs in fluorous phases [47]. These fluorous-soluble catalysts were found to have high activity for the hydrogenation of alkenes when the two phases are mixed. Most importantly, the catalyst can be easily recovered by allowing the two phases to separate, and they could be recycled up to 12 times without appreciable loss of catalytic activity.

We were also able to covalently link perfluoroether groups onto the surface of PPI dendrimers and thereafter prepare encapsulated Pd nanoparticles [50]. These DEMNs catalyzed the Heck reaction between iodobenzene and *n*-butyl acrylate in a fluorous/hydrocarbon solvent to yield *n*-butyl trans-formylcinnamate with 100% regioselectivity at 90 °C. No leaching of metal from the dendrimer was observed, but the original activity of the catalysts was not fully recovered.

7. Heterogeneous catalysis

Because of the ease of separating catalysts from substrates and products, heterogeneous catalysts are very commonly used in industrial processes. However, catalysts supported on silica, alumina, or highly cross-linked polymer beads often suffer from diminished activity compared to their homogeneous analogues due to limited accessibility [77]. Thus, immobilization of nanoparticles onto solid supports is a crucial step in fabrication of practical heterogeneous catalysts.

Because of potential applications of DEMNs as heterogeneous catalysts, we studied the electrocatalytic properties of DEMNs for O$_2$ reduction. Such studies have potential applications to fuel cells [33]. In the presence of O$_2$, a G4-OH(Pt$_{60}$)-modified Au electrode reveals a much higher current and a positive shift in the onset potential for oxygen reduction compared to a G4-OH-modified Au electrode lacking the encapsulated Pd nanoparticles. These results are consistent with substantial catalytic activity. Pd nanoparticles can also be immobilized onto flat surfaces, such as mica and highly orient pyrolytic graphite (HOPG) [78]. Surface modification can be accomplished either by direct adsorption of DEMNs, or by first adsorbing the empty dendrimer and then synthesizing the nanoparticle in

situ. In both cases, it is possible to use the materials as heterogeneous catalysts.

It is also possible to remove the dendrimer template after sorption of DEMNs onto mica or HOPG supports, but in this case aggregation of nanoparticles was observed. The use of different supports, such as silica, would provide a better platform for stabilizing the nanoparticles after removal of the dendrimer template. For example, silica-PAMAM dendrimer hybrids have been prepared by first modifying the dendrimer with 3-(trimethoxysilyl) propyl acrylate, and then reacting this material with partly hydrolyzed tetraethylorthosilicate [79]. Condensation of this material yielded the final composite material, which exhibited a high metal-ion complexation capacity, presumably due to the presence of the dendrimer. Although the authors did not reduce the resulting material, one could easily imagine doing so thereby obtaining DEMNs for catalyst applications.

8. Conclusions and outlook

This account has described the synthesis and application of dendrimer-encapsulated monometallic and bimetallic nanoparticles to catalysis. These materials have proven to be highly effective homogeneous catalysts for reactions ranging from simple hydrogenations to more sophisticated Heck and Suzuki reactions. Independent of the type or generation of dendrimer template in which they are synthesized, DEMNs are among the most monodisperse 1–4 nm metal particles thus far reported. One of the most promising aspects of DEMNs is that the dendrimer fraction of the composite can be tailored to induce substrate or product selectivity. Likewise, the periphery of the dendrimer can be configured to render DEMNs soluble in solvents ranging from water to supercritical CO_2, or to attach the dendrimers to surfaces for applications to heterogeneous catalysis.

Although dendrimers are relatively expensive compared with other commercial catalysts, we have shown that they can be easily recovered and recycled which perhaps makes it possible to consider the use of DEMNs for some real-world applications. An alternative is to use DEMNs as model systems to study structure-function relationships, and then devise methods to incorporate the same functions into nanoparticles encapsulated within inexpensive star or hyperbranched polymers.

Because of the unique and easily tunable properties of DEMNs, and because of their high degree of uniformity, DEMNs may find applications beyond catalysis. For example, they could be used as tags for bioassays, as active components in nanoelectronics, and as magnetic materials for data storage. For example, Dickson et al. have shown that DEMNs containing just a few Ag atoms are highly fluorescent [25], and Dai et al. have demonstrated that single-walled carbon nanotubes having very narrow diameter distributions can be templated by DEMNs [80].

References

[1]　G.R. Newkome, C.N. Moorefield, F. Vögtle, Dendritic Macromolecules: Concepts, Synthesis, Perspectives, Wiley-VCH, Weinheim, Germany, 1996.

[2]　E. Buhleier, W. Wehner, F. Vögtle, Synthesis (1978) 155.

[3]　D. Astruc, F. Chardac, Chem. Rev. 101 (2001) 2991.

[4]　A.W. Bosman, R.A.J.J. Jansen, E.W. Meijer, Chem. Rev. 99 (1999) 1665.

[5]　R.M. Crooks, M. Zhao, L. Sun, V. Chechik, L.K. Yeung, Acc. Chem. Res. 34 (2001) 181.

[6]　J.M.J. Fréchet, Proc. Natl Acad. Sci. USA 99 (2002) 4782.

[7]　R. van Heerbeek, P.C.J. Kamer, P.W.N.M. van Leeuwen, J.N.H. Reek, Chem. Rev. 102 (2002) 3717.

[8]　F. Vögtle, S. Gestermann, R. Hesse, H. Schwierz, B. Windisch, Prog. Polym. Sci. 25 (2000) 987.

[9]　S.C. Zimmerman, L.J. Lawless, Top. Curr. Chem. 217 (2001) 95.

[10]　F. Zeng, S.C. Zimmerman, Chem. Rev. 97 (1997) 1681.

[11]　A.K. Patri, I.J. Majoros, J.R. Baker Jr, Curr. Opin. Chem. Biol. 6 (2002) 466.

[12]　C. Kojima, K. Kono, K. Maruyama, T. Takagishi, Bioconjugate Chem. 11 (2000) 910.

[13]　A. Adronov, J.M.J. Fréchet, Chem. Commun. 18 (2000) 1701.

[14]　A. Adronov, S.L. Gilat, J.M.J. Fréchet, K. Ohta, F.V.R. Neuwahl, G.R. Fleming, J. Am. Chem. Soc. 122 (2000) 1175.

[15] S.F. Swallen, Z.G. Zhu, J.S. Moore, R. Kopelman, J. Phys. Chem. B 104 (2000) 3988.

[16] M.W.P.L. Baars, E.W. Meijer, Host-Guest Chemistry of Dendritic Molecules, Top. Curr. Chem. 210 (2000) 131.

[17] L.J. Twyman, A.S.H. King, J. Chem. Res. S 2 (2002) 43.

[18] L.J. Twyman, A.S.H. King, I.K. Martin, Chem. Soc. Rev. 31 (2002) 69.

[19] G.E. Oosterom, J.N.H. Reek, P.C.J. Kamer, P.W.N.M. Van Leeuwen, Angew. Chem. Int. Ed. Engl. 40 (2001) 1828.

[20] R. Kreiter, A.W. Kleij, R.J.M.K. Gebbink, G. van Koten, Top. Curr. Chem. 217 (2001) 163.

[21] M. Zhao, L. Sun, R.M. Crooks, J. Am. Chem. Soc. 120 (1998) 4877.

[22] F. Gröhn, B.J. Bauer, Y.A. Akpalu, C.L. Jackson, E.J. Amis, Macromolecules 33 (2000) 6042.

[23] K. Esumi, A. Suzuki, A. Yamahira, K. Torigoe, Langmuir 16 (2000) 2604.

[24] O. Varnavski, R.G. Ispasoiu, L. Balogh, D. Tomalia, T. Goodson III, J. Chem. Phys. 114 (2001) 1962.

[25] J. Zheng, R.M. Dickson, J. Am. Chem. Soc. 124 (2002) 13982.

[26] R.W.J. Scott, A.K. Datye, R.M. Crooks, J. Am. Chem. Soc. 125 (2003) 3708.

[27] B.I. Lemon III, R.M. Crooks, J. Am. Chem. Soc. 122 (2000) 12886.

[28] M.F. Ottaviani, F. Montalti, M. Romanelli, N.J. Turro, D.A. Tomalia, J. Phys. Chem. 100 (1996) 11033.

[29] M. Zhao, R.M. Crooks, Chem. Mater. 11 (1999) 3379.

[30] P.N. Floriano, C.O. Noble, J.M. Schoonmaker, E.D. Poliakoff, R.L. McCarley, J. Am. Chem. Soc. 123 (2001) 10545.

[31] A.W. Bosman, A.P.H.J. Schenning, R.A.J.J. Janssen, E.W. Meijer, Chem. Ber./Recueil 130 (1997) 725.

[32] M. Zhao, R.M. Crooks, Angew. Chem. Int. Ed. Engl. 38 (1999) 364.

[33] M. Zhao, R.M. Crooks, Adv. Mater. 11 (1999) 217.

[34] L. Zhou, D.H. Russell, M. Zhao, R.M. Crooks, Macromolecules 34 (2001) 3567.

[35] Y. Niu, L. Sun, R.M. Crooks, Macromolecules 36 (2003) 5725.

[36] L. Sun, R.M. Crooks, J. Phys. Chem. B 106 (2002) 5864.

[37] V. Chechik, M. Zhao, R.M. Crooks, J. Am. Chem. Soc. 121 (1999) 4910.

[38] A.C. Curtis, D.G. Duff, P.P. Edwards, D.A. Jefferson, B.F.G. Johnson, A.I. Kirkland, A.S.A. Wallace, Angew. Chem. Int. Ed. Engl. 27 (1988) 1530.

[39] I. Lisiecki, M.P. Pileni, J. Am. Chem. Soc. 115 (1993) 3887.

[40] Y. Niu, L.K. Yeung, R.M. Crooks, J. Am. Chem. Soc. 123 (2001) 6840.

[41] Y. Li, M.A. El-Sayed, J. Phys. Chem. B 105 (2001) 8938.

[42] S.-K. Oh, Y. Niu, R.M. Crooks (in preparation).

[43] Y. Kawazoe, T. Kondow, K. Ohno, Clusters and Nanomaterials: Theory and Experiment, Springer, Berlin, 2002.

[44] G. Schmid, Clusters and Colloids: From Theory to Applications, VCH, Weinheim, Germany, 1994.

[45] Y.-G. Ki, S.-K. Oh, R.M. Crooks, Nano Lett. (submitted).

[46] Y.-G. Ki, S.-K. Oh, Y.-G. Kim, H. Ye, R.M. Crooks, Langmuir (in press).

[47] V. Chechik, R.M. Crooks, J. Am. Chem. Soc. 122 (2000) 1243.

[48] Y. Sayed-Sweet, D.M. Hedstrand, R. Spinder, D.A. Tomalia, J. Mater. Chem. 7 (1997) 1199.

[49] K. Esumi, T. Hosoya, A. Suzuki, K. Torigoe, J. Colloid Interface Sci. 229 (2000) 303.

[50] L.K. Yeung, R.M. Crooks, Nano Lett. 1 (2001) 14.

[51] K. Esumi, R. Nakamura, A. Suzuki, K. Torigoe, Langmuir 16 (2000) 7842.

[52] Y. Niu, R.M. Crooks, Chem. Mater. 15 (2003) 3463–3467.

[53] J.C. Garcia-Martinez, R.W.J. Scott, R.M. Crooks, J. Am. Chem. Soc. 125 (2003) 11190–11191.

[54] B.C. Gates, Chem. Rev. 95 (1995) 511.

[55] H. Hirai, J. Macromol. Sci.–Chem. A 13 (1979) 633.

[56] J. Kiwi, M. Graetzel, J. Am. Chem. Soc. 101 (1979) 7214.

[57] A.C. Templeton, W.P. Wuelfing, R.W. Murray, Acc. Chem. Res. 33 (2000) 27.

[58] M. Brust, J. Fink, D. Bethell, D.J. Schiffrin, C. Kiely, Chem. Commun. 16 (1995) 1655.

[59] M.-P. Pileni, Supramol. Sci. 5 (1998) 321.

[60] M. Králik, A. Biffis, J. Mol. Catal. A–Chem. 177 (2001) 113.

[61] A.B.R. Mayer, Polym. Adv. Technol. 12 (2001) 96.

[62] P.N. Rylander, Catalytic Hydrogenation in Organic Syntheses, Academic Press, New York, 1979.

[63] P.N. Rylander, Catalysis in Organic Syntheses, Academic Press, New York, 1980.

[64] M. Chai, Y. Niu, W.J. Youngs, P.L. Rinaldi, J. Am. Chem. Soc. 123 (2001) 4670.

[65] M. Murat, G.S. Grest, Macromolecules 29 (1996) 1278.

[66] P.G. Jessop, T. Ikariya, R. Noyori, Chem. Rev. 99 (1999) 475.

[67] L.K. Yeung, C.J. Lee Jr, K.P. Johnston, R.M. Crooks, Chem. Commun. (2001) 2290.

[68] C.L. Jackson, H.D. Chanzy, F.P. Booy, B.J. Drake, D.A. Tomalia, B.J. Bauer, E.J. Amis, Macromolecules 31 (1998) 6259.

[69] A. Hierlemann, J.K. Campbell, L.A. Baker, R.M. Crooks, A.J. Ricco, J. Am. Chem. Soc. 120 (1998) 5323.

[70] H. Tokuhisa, M. Zhao, L.A. Baker, V.T. Phan, D.L. Dermody, M.E. Garcia, R.F. Peez, R.M. Crooks, T.M. Mayer, J. Am. Chem. Soc. 120 (1998) 4492.

[71] Y. Niu, J. Alvarez, R.M. Crooks (unpublished results).

[72] I.T. Horváth, J. Raba, Science 266 (1994) 72.

[73] B. Richter, A.L. Spek, G. van Koten, B.-J. Deelman, J. Am. Chem. Soc. 122 (2000) 3945.

[74] J.L. Kendall, D.A. Canelas, J.L. Young, J.M. DeSimone, Chem. Rev. 99 (1999) 543.

[75] J.A. Darr, M. Poliakoff, Chem. Rev. 99 (1999) 495.

[76] H.P. Dijkstra, G.P.M. van Klink, G. van Koten, Acc. Chem. Res. 35 (2002) 798.

[77] K. Inoue, Prog. Polym. Sci. 25 (2000) 453.

[78] L. Sun, R.M. Crooks, Langmuir 18 (2002) 8231.

[79] E. Ruckenstein, W. Yin, J. Polym. Sci. Part A: Polym. Chem. 38 (2000) 1443.

[80] H.C. Choi, W. Kim, D. Wang, H. Dai, J. Phys. Chem. B 106 (2002) 12361.